Tellus (1995), 47A, 473–494
Printed in Belgium – all rights reserved

TELLUS
ISSN 0280–6495

Climate variability in a low-order coupled atmosphere-ocean model

By PAUL J. ROEBBER*, *Department of Atmospheric Science, State University of New York at Albany, Albany, New York, USA*

(Manuscript received 12 April 1994; in final form 21 November 1994)

ABSTRACT

The dynamical behavior of the climate system is investigated through the use of a low-order coupled atmosphere-ocean general circulation model. The goal is to gain some qualitative understanding of how non-linear interactions between the individual system components may affect the climate. Both the atmosphere and ocean models are fully dynamic: the former is defined by 3 ordinary differential equations derived from a truncated Fourier series expansion of the mean and perturbation components of the quasi-geostrophic potential vorticity equation, while the latter is specified by 6 ordinary differential equations representing the time-dependent variations of ocean temperature and salinity in a 3-box model of the North Atlantic. Despite the existence of 2 basic equilibrium ocean model responses to perpetual atmospheric conditions, equilibrium states are never attained in the coupled system within 10000 years of integration; the deep ocean flow continually adjusts to the atmospheric regime changes associated with particular ocean circulations, which leads to new circulations and new atmospheric regimes. Low-frequency quasi-periodic oscillations about a single state of the thermohaline circulation result from an advective-diffusive process, modulated by the correlation of the atmospheric behavior with the phase of the ocean cycle. The climate is strongly effected by interactions with the ocean, leading to distinct atmospheric patterns for different phases in the oscillations, and a conversion of some of the high-frequency atmospheric signal to lower frequencies. This conversion also results in a measurable ocean response at high frequencies. Furthermore, owing to the richness of the atmospheric response to small modifications in the meridional and zonal gradients in diabatic heating, even modest adjustments in the ocean circulation resulting from interactions with the high-frequency atmospheric component can also lead to climate change over relatively short time periods. The results of the model are applied to recent deductions of climate variability in the North Atlantic, obtained from Greenland ice-cores.

1. Introduction

Since the response time of the atmosphere is much shorter than that of the oceans, and because the atmosphere and oceans are strongly coupled through exchanges of energy, momentum and water mass, the high-frequency or "white-noise" atmospheric signal tends to produce a low-frequency oceanic response, over time spans ranging from decades to centuries (Hasselmann, 1976). However, a complete representation of the atmosphere-ocean coupling must include not only this "stochastic" atmospheric forcing, but also the feedback from the ocean to the atmosphere and then the subsequent interaction from the atmosphere back to the ocean. Hasselmann (1982) proposed that this interaction could be modeled as a superposition of a "white-noise" random atmospheric forcing and a linear feedback loop, in which variations of the sea surface properties would induce variations in the mean atmospheric circulation, which in turn would yield changes in the mean and "white-noise" atmospheric forcing of the ocean. In conventional terms, one component of climate

* Current affiliation: Department of Geosciences, University of Wisconsin at Milwaukee, Milwaukee, Wisconsin, USA.

variability would then be a linear atmospheric response to the slowly varying conditions imposed by the oceans at the lower boundary.

However, the response of the atmosphere-ocean climate subsystem to the two-way interactions between transient atmospheric circulations and the deep ocean flow is likely quite complex. The atmosphere, like many non-linear systems, may display a range of dynamic behaviors, including fully chaotic vacillations (Lorenz, 1984; 1990), while the deep ocean circulation might display almost-intransitive behavior, that is, it might undergo variations on a range of time-scales between two or more states of quasi-equilibrium. This latter idea has been supported by a number of investigations (Stommel, 1961; Rooth, 1982; Bryan, 1986ab; Marotzke et al., 1988). Under such conditions, internal changes in the atmosphere-ocean system, such as the "white-noise" forcing of the atmosphere, could drive the ocean towards a new quasi-equilibrium state (Mikolajewicz and Maier-Reimer, 1990). Such changes in the oceans impose new boundary conditions on the atmosphere, leading to new atmospheric behaviors, which would result in new changes in the atmospheric forcing of the ocean. As a consequence, it is not likely that the feedback from the ocean to the atmosphere would be linear.

Accordingly, the behavior of a fully dynamic coupled atmosphere-ocean system is investigated, in order to gain some understanding of how such interactions might effect the circulations of the two sub-systems. In order to achieve such an ambitious goal, these investigations are restricted to the dynamics of a low-order atmosphere-ocean general circulation model of the North Atlantic. As discussed by Lorenz (1982, 1984), such models serve principally as a means for examining hypotheses in a more rigorous manner than is afforded by qualitative reasoning alone, since the non-linearity of the interactions renders it difficult to make a priori predictions of system behavior on the basis of such reasoning. As such, specific quantitative information obtained from integrations of the system must be viewed in a rather general way. Despite this reservation, it is believed that such investigations have an important role to play in understanding atmosphere-ocean dynamics. A number of studies have examined coupled atmosphere-ocean models in the context of energy balance formulations of the atmosphere (Birchfield et al., 1990; Harvey, 1992; Stocker et al., 1992). A unique aspect of this work is that the atmospheric model incorporates a range of high-frequency non-linear dynamical behaviors, and so the effect of such circulations on the coupled system can be directly studied.

2. The atmospheric model

2.1. Model structure

Lorenz (1984, 1990) introduced a low-order atmospheric "general circulation" model, defined by three ordinary differential equations:

$$\frac{\mathrm{d}X}{\mathrm{d}t} = -Y^2 - Z^2 - aX + aF, \tag{1}$$

$$\frac{\mathrm{d}Y}{\mathrm{d}t} = XY - bXZ - Y + G, \tag{2}$$

$$\frac{\mathrm{d}Z}{\mathrm{d}t} = bXY + XZ - Z. \tag{3}$$

Although not shown by Lorenz, these equations can be derived from the mean and perturbation quasi-geostrophic potential vorticity equations (Holton, 1992, p. 164–165), using a truncated Fourier series expansion of the geostrophic streamfunction. The independent variable t represents time, while X, Y and Z represent the meridional temperature gradient (or equivalently from thermal wind balance, the strength of the zonal flow), and the amplitudes of the cosine and sine phases of a chain of superposed large scale eddies, respectively.

In eq. (1), F represents the meridional gradient of diabatic heating, and is the value to which X would be driven (over some damping time proportional to a^{-1}) in the absence of coupling between the westerly current and the eddies. The term G in eq. (2) is the asymmetric thermal forcing, representing the longitudinal heating contrast between land and sea, and is the value to which Y would be driven (over a damping time of unity) in the absence of coupling. This coupling, which results in amplification of the eddies at the expense of the westerly current, is represented by the quadratic terms XY in eq. (2), XZ in eq. (3) and $-Y^2-Z^2$ in eq. (1). This can be seen more clearly by casting (1)–(3) in an energy form:

$$\frac{dX^2}{dt} = -2X(Y^2+Z^2) - 2aX^2 + 2aXF, \tag{4}$$

$$\frac{d(Y^2+Z^2)}{dt} = 2X(Y^2+Z^2) - 2(Y^2+Z^2) + 2YG, \tag{5}$$

where eqs. (4) and (5) are proportional to the mean and perturbation energies, respectively. The total energy of the system, which is proportional to the sum of (4) and (5), is the sum of the diabatic generation terms (involving F and G) and the dissipation terms (involving $-X^2$ and $-Y^2-Z^2$), since the first term on the right-hand sides of (4) and (5), which represents the amplification of the eddies at the expense of the westerly current, exactly cancels. Finally, the quadratic terms proportional to b in (2) and (3) represent displacement of the eddies by the westerly current. Thus, for $a<1$ and $b>1$, the eddies damp more rapidly than the westerly flow and are displaced more rapidly than they amplify.

2.2. *Time-dependent behavior*

Lorenz (1984) showed that for special values of the asymmetric thermal forcing G, the equations display chaotic behavior for perpetual "winter" conditions, and intransitive behavior for perpetual "summer" conditions, with the winter/summer seasons defined by fixed values of the meridional gradient of diabatic heating F. Lorenz (1990) showed that when F is allowed to vary in a seasonal cycle between the winter and summer values, interannual variability is evident, with chaotic winters followed by irregular alternations between "active" and "inactive" summers, so characterized by strong or weak oscillations in the intensity of the westerly current, respectively. Lorenz (1990) identified the mechanism that produces these variations: the chaotic winter behavior assures essentially random "initial" conditions at the onset of the summer, so that either of the two persistent summer circulation patterns may develop. In that paper, it was also noted that a seasonal cycle should be expressed in G as well as F, since at a given latitude, the land is generally colder (warmer) than the sea in winter (summer). Masoller et al. (1992) also studied the system defined by eq. (1)–(3) with G fixed and F variable. These studies indicate that the asymmetry between the oceans and continents represented by G plays a fundamental rôle in generating the complex dynamical behavior of the model.

However, the behavior of this system as a function of concurrent variations in both of the diabatic heating terms (F and G) has not been extensively studied. This issue is of some importance to the present study, since the longer-term coupling between the atmosphere and ocean takes place through both of these parameters; variations in the transport of heat by the ocean (and consequently ocean surface temperatures) will lead to variations in both the meridional and asymmetric thermal forcing, superimposed upon the seasonal cycle.

Consequently, numerical solutions of eqs. (1)–(3) will be examined as a function of a range of (fixed) values of F and G. For these solutions, numerical integrations have been carried out using a fourth-order Runge-Kutta scheme, with a time increment of 0.025 units (corresponding to 3 h). Following Lorenz (1984, 1990), the model parameters a and b are fixed at 0.25 and 4, respectively, for all simulations in this paper. The damping time (resulting from radiative and mechanical dissipation) for the waves is chosen as the time unit, representing 5 days; as discussed above, this choice of parameters means that the meridional temperature gradient damps more slowly, in 20 days.

Fig. 1 shows the variations of X for $F=6$ and two values of G representing perpetual "summer" conditions. For $G=-1$, intransitivity prevails, with the two states representing the "active" (Fig. 1a) and "inactive" (Fig. 1b) summer conditions discussed by Lorenz (1990). When G is decreased to -1.25 (representing an increase in the zonal gradient of diabatic heating, with the land warmer than the sea), intransitivity continues, but now the two stable solutions are different. The conditions displayed in Fig. 1c represent a modified "inactive" flow while those of Fig. 1d correspond to an atmospheric "blocking" regime, analogous to solution D from Fig. 1 of Lorenz (1984). Further analysis reveals that the intransitivity continues until $G \approx -1.4$, at which point only the blocking solution remains.

It should be noted that the pattern indicated by Fig. 1d and eqs. (1)–(3) differs from the classical picture of an atmospheric block (characterized by a large-scale equivalent barotropic structure and consequently little *direct* meridional heat trans-

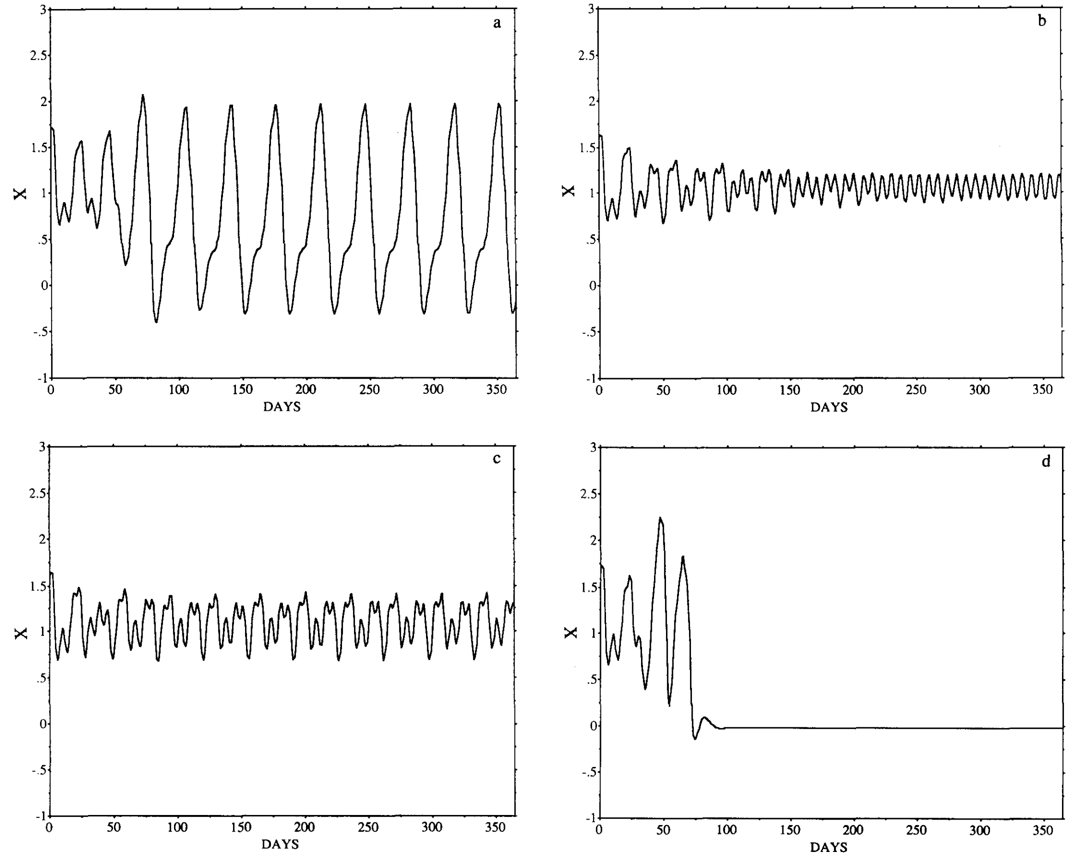

Fig. 1. Atmospheric meridional temperature gradient (X) for perpetual summer conditions ($F = 6$) with initial values of (a) $G = -1$, $X = 1.7$, $Y = 0$, $Z = 0$ and (b) $G = -1$, $X = 1.6$, $Y = 0$ and $Z = 0$, (c) $G = -1.25$, $X = 1.6$, $Y = 0$, $Z = 0$ and (d) $G = -1.25$, $X = 1.7$, $Y = 0$ and $Z = 0$.

port). Lorenz (1990) noted that eqs. (1)–(3) assume a westward tilt with height; here, the "block" is a stationary wave that itself transports a considerable amount of heat poleward, in order to balance the meridional gradient of diabatic heating in the absence of significant dissipation. However, real atmospheric blocks, as a consequence of the "steering" of synoptic-scale eddies (Blackmon et al., 1986), can nonetheless be associated with considerable heat transport (Palmén and Newton, 1969, pp. 274–278; Mullen, 1986), as for instance with the "Viererdruckfeld" pattern described by Raethjen (1949). Rex (1950ab) noted that such transitions from transient zonal to quasi-stationary and persistent meridional atmospheric circulations occur at a well-defined longitude in the North Atlantic and that significant climatic anomalies (in temperature and precipitation) over the Atlantic and Europe are associated with their development. Consequently, the term "block" will be used in the remainder of this paper to denote these stationary wave patterns.

The solutions for perpetual "winter" conditions (with F fixed at 8) are much different. As discussed in Lorenz (1984, 1990), intransitivity appears near $G = 0.8$. The first solution contains double wave passages ("weak" followed by "strong") with each oscillation of the meridional temperature gradient, while the second solution takes a form reminiscent of atmospheric "index cycles". The transition to chaotic dynamics occurs at about $G = 0.9$, and this behavior continues until $G = 1.36$, where the solution becomes briefly periodic again. For values of G greater than 1.36, the blocking solution appears.

Thus, variations in G for fixed F lead to a wide range of possible behaviors.

It is possible to more concisely summarize the atmospheric model behavior by categorizing the attractors themselves as a function of both F and G. One can think of a small sphere that is initially placed about some point of the attractor, whose phase-space position is defined by the three model variables (X, Y, Z). If each point of the sphere is then allowed to follow its orbit in phase-space for a sufficiently long time, the initial sphere will be deformed into an approximate ellipsoid. The growth rate of the ellipsoid axes are defined by the so-called Lyapunov exponents (Bergé et al., 1984; Wolf et al., 1985), which therefore describe the mean rate of exponential divergence of initially neighboring trajectories. The signs of the spectrum of Lyapunov exponents allow one to categorize the type of attractor being studied. Bergé et al. (1984) noted that for a 3-dimensional dynamical system, the possible Lyapunov spectra and associated attractors are: $(-, -, -)$ fixed point or steady state solution; $(0, -, -)$ limit cycle or periodic solution; $(0, 0, -)$ T^2 torus, leading to a quasi-periodic solution; $(+, 0, -)$ strange attractor yielding chaotic behavior.

Using the method of Wolf et al. (1985), the Lyapunov spectra as a function of fixed values of F and G have been calculated for the atmospheric model by integrating eq. (1)–(3) for 20-year periods for an ensemble of random initial conditions for each F, G pair. The resulting attractor classifications are presented in Table 1, which is meant to be used as a coarse, qualitative guide

Table 1. *Characterization of atmospheric model attractors as a function of F and G*

	$F=3.0$	$F=4.0$	$F=5.0$	$F=6.0$	$F=7.0$	$F=8.0$	$F=9.0$
$G=-1.4$	fixed pt	fixed pt	fixed pt	limit fixed pt	fixed pt	fixed pt	strange
$G=-1.3$	fixed pt	fixed pt	fixed pt	limit fixed pt	limit fixed pt	strange	strange
$G=-1.2$	fixed pt	fixed pt	fixed pt	limit fixed pt	limit	limit	limit
$G=-1.1$	limit fixed pt	fixed pt	limit fixed pt	limit limit	strange	strange	limit
$G=-1.0$	limit fixed pt	limit fixed pt	limit	limit limit	limit	strange	limit
$G=-0.9$	fixed pt	limit	limit	limit limit	limit	strange	limit
$G=-0.8$	limit limit	limit limit	limit	limit	limit	limit	strange
—	—	—	—	—	—	—	—
$G=0.8$	limit	limit	limit	limit	limit	limit	limit strange
$G=0.9$	fixed pt	limit	limit	limit	limit	strange	limit
$G=1.0$	fixed pt	fixed pt	strange	limit	limit	strange	limit
$G=1.1$	limit fixed pt	fixed pt	fixed pt	limit	strange	strange	limit
$G=1.2$	fixed pt	fixed pt	fixed pt	limit	limit	strange	strange
$G=1.3$	fixed pt	fixed pt	fixed pt	fixed pt	limit	strange	strange
$G=1.4$	fixed pt	fixed pt	fixed pt	fixed pt	limit fixed pt	fixed pt	strange

concerning the solution changes in $F-G$ space. That Table 1 is not comprehensive can be appreciated by considering that Masoller et al. (1992) found that for $G=1$, the dynamical behavior was highly complex within relatively narrow windows in F ($\Delta F \ll 1.0$). Such changes, as noted above, can also occur for relatively small variations in G for fixed F. Multiple entries at a particular $F-G$ coordinate in Table 1 denote intransitivity, although the attractor types themselves need not be distinct (e.g., limit, limit indicates 2 distinct periodic solutions were found, as for instance would denote the active/inactive states for $F=6$ and $G=-1$).

In a broader context, one can consider "summer" conditions to be represented by small F and $G<0$, while "winter" conditions are consistent with large F and $G>0$. Scanning the entries in Table 1, it is apparent that in summer, the circulations correspond to periodic or steady (blocking) solutions, and that intransitivity is common. In winter, the circulations correspond to chaotic, periodic or steady (blocking) solutions; intransitivity exists but is less common than in summer. Thus, the seasonal "climates" as defined by the attractors are quite distinct and the climate response to the ocean feedback (as expressed through F and G) is highly complex and non-linear. This issue will be addressed again, in Subsection 4.1, in the context of the atmospheric coupling to the ocean model.

3. The ocean model

The goal is to construct a qualitatively correct low-order model of the thermohaline circulation of the North Atlantic ocean. By limiting the study to a single ocean basin, the results obtained will not address the *global* dynamics of the interaction of the atmosphere with the deep ocean circulation. Inclusion of more basins would account for the specific differences of the global deep ocean circulation from that of the individual basins, shown by Marotzke (1990) and Wright and Stocker (1991) to result from inter-basin interactions. However, as will be shown in Sections 4 and 5, the dynamics of the single-hemisphere coupled model are sufficiently complex and interesting to warrant its study before proceeding to more complicated designs.

The thermohaline circulation, in its simplest form, is characterized by a meridional overturning flow; relatively warm surface waters flow northward and cool at high latitudes, sink due to a loss of buoyancy, and spread southward at depth. The circuit is completed by a slow, broad upwelling of the deep, southward flowing water. This purely temperature driven flow is easily modified by consideration of the contribution of salinity to the overall buoyancy; thus, the additional effect of the exchange of water mass through the processes of precipitation and evaporation must also be considered.

A number of approaches to modelling such a flow are imaginable. For instance, it should be possible to characterize the ocean circulation in the form of a meridional plane model, with a streamfunction proportional to the horizontal gradients of salinity and temperature. In a procedure analogous to the derivation of the atmospheric model, the fields of temperature (T) and salinity (S) could then be represented in terms of a truncated Fourier series expansion, yielding time-dependent equations for the evolution of the Fourier components. An example of such an approach is given by Källén and Huang (1987). However, because of the vertical structure of T and S in even a simple thermohaline model (e.g., Marotzke et al., 1988), such an expansion involves a relatively large number of terms and is therefore not consistent with the stated aim of relative simplicity.

However, a wide variety of so-called box models have been used to study the qualitative dynamics of the thermohaline circulation (see Weaver and Hughes, 1992 for a review). In these models, the ocean is represented as a series of interconnected reservoirs in which T and S are thoroughly mixed and flow between the boxes is directly proportional to the horizontal density gradient. The box model approach is attractive for the purposes of this study since such models are conceptually simple, provide a reasonable, qualitative representation of the thermohaline circulation (with surface flow towards regions of higher density and return flow at depth) and can represent higher order, nonlinear behavior such as multiple equilibria and self-sustained oscillations (Stommel, 1961; Welander, 1982), behaviors that are also evident in more complicated zonally averaged models (Marotzke et al., 1988; Wright and Stocker, 1991). Furthermore, their limitations are well understood.

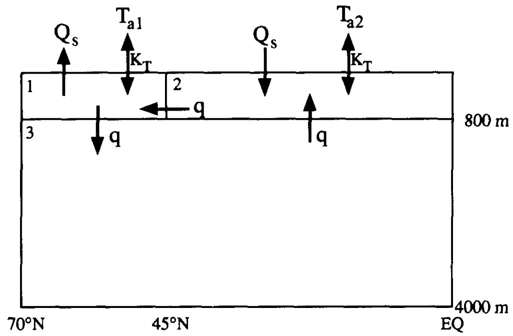

Fig. 2. The geometry of the North Atlantic 3 box model. Q_s denotes the equivalent salt flux (differential net surface evaporation), T_{A_1} and T_{A_2} represent restoring air temperatures with restoring constant K_T, and q is the magnitude of the thermohaline circulation. The sense of the circulation indicated denotes q positive.

The ocean model adopted here is closely related to the 3-box model of the North Atlantic thermohaline circulation presented by Birchfield (1989). The basic geometry of the ocean model is shown in Fig. 2. The North Atlantic, which is considered to be isolated from the rest of the world ocean, is represented by a deep ocean box and two near-surface boxes, the latter boxes extending from the equator to 45° N, and then from 45° N to 70° N. The ocean depth is fixed at 4 km, with the surface boxes 800 m deep. As in Birchfield (1989), the ocean model is forced by differential heating and net evaporation at the surface. However, this forcing is represented here as a restoring law on temperature and a flux boundary condition on salinity. In addition, to limit the number of free parameters, horizontal eddy mixing is neglected. A further extension of this study might involve the incorporation of horizontal eddy mixing, which could crudely represent the effects of the wind-driven ocean circulation on the large-scale meridional overturning flow (Birchfield, 1989). The horizontal eddy mixing coefficients could then be coupled to the atmospheric model through the mean zonal wind X, representing the mid-latitude component of the wind-stress curl.

With the application of conservation of heat, salt and water mass, the equations describing T and S in the 3-box model become:

$$V_1 \frac{dT_1}{dt} = \frac{1}{2} q(T_2 - T_3) + K_T(T_{A_1} - T_1) - K_{Z_1}(T_1 - T_3), \tag{6}$$

$$V_2 \frac{dT_2}{dt} = \frac{1}{2} q(T_3 - T_1) + K_T(T_{A_2} - T_2) - K_{Z_2}(T_2 - T_3), \tag{7}$$

$$V_3 \frac{dT_3}{dt} = \frac{1}{2} q(T_1 - T_2) + K_{Z_1}(T_1 - T_3) + K_{Z_2}(T_2 - T_3), \tag{8}$$

$$V_1 \frac{dS_1}{dt} = \frac{1}{2} q(S_2 - S_3) - K_{Z_1}(S_1 - S_3) - Q_s, \tag{9}$$

$$V_2 \frac{dS_2}{dt} = \frac{1}{2} q(S_3 - S_1) - K_{Z_2}(S_2 - S_3) + Q_s, \tag{10}$$

$$V_3 \frac{dS_3}{dt} = \frac{1}{2} q(S_1 - S_2) + K_{Z_1}(S_1 - S_3) + K_{Z_2}(S_2 - S_3), \tag{11}$$

where q in eqs. (6)–(11) is the thermohaline circulation with the flow as indicated in Fig. 2 denoted by positive values. V_j is the box volume, T_j and S_j denote the volume average temperature and salinity, and K_{Z_j} is the vertical eddy mixing coefficient of box j. K_T is the temperature restoring constant, such that V/K_T gives a restoring timescale (see below), and Q_s is the volume averaged equivalent salt flux, proportional to the differential net surface evaporation.

Birchfield (1989) argued that the magnitude of the thermohaline circulation should be determined by the local production of dense water, which would tend to increase the mean density of the box. Since the vertical density gradients in boxes 1 and 2 are both proportional to the density of the deep water box as well as the density of the surface box, the thermohaline circulation can then be defined by:

$$q = \frac{\mu}{\rho_0} (\rho_1 - \rho_2), \tag{12}$$

where a linear equation of state is assumed and μ is a hydraulic transport coefficient. The choice of $\mu = 4 \times 10^{10}$ m^3 s^{-1} gives the appropriate order of magnitude for the North Atlantic thermohaline circulation (e.g., Gordon, 1986). It should be noted that the form of eq. (12) is typical of box models in that the thermohaline circulation is decoupled from the process of convection and deep water formation. However, the more sophisticated zonally-averaged ocean model of Wright and Stocker (1991) also leads to a form for the meridional transport like eq. (12), that is, the flow is ultimately driven by the meridional pressure (density) gradient.

The vertical eddy diffusion coefficients K_{Z_1} and K_{Z_2} are set to $5.276 \times 10^5\ \mathrm{m^3\,s^{-1}}$, which yields an equivalent time-scale of O(500–1000 years) for the surface boxes, a value consistent with diffusive processes. Analysis of eqs. (6)–(11) reveals that large-scale gravitational stability is not guaranteed; in particular, for the case of collapsed flows ($q \approx 0$), convective overturning should eventually occur in response to increasing low-latitude surface salinity. Consequently, the vertical density gradients between the surface and deep boxes are computed at each time step; in case of large-scale static instability, the vertical eddy diffusion coefficient is increased by a factor of 10^3. This approach is consistent with convective adjustment procedures that have appeared elsewhere (Cox, 1984; Weaver and Sarachik, 1990).

In models with a Newtonian boundary condition on temperature, the upper layer of the ocean is restored to an appropriate reference temperature on a fast time-scale of the order of 1–2 months. A typical choice of a restoring time-scale for a 50 m surface layer is 30 days (Marotzke and Willebrand, 1991). In the present model, neglecting advection and with $K_T \gg K_{Z_1}$, the solution to eq. (6) can be written as:

$$T_1(t) = T_{A_1} + [T_1(0) - T_{A_1}] \exp\left(-\frac{K_T}{V_1} t\right), \quad (13)$$

where T_{A_1} is the restoring temperature and the term V_1/K_T is the restoring time-scale. Eq. (13) indicates that the *volume* average temperature of box 1 should be restored to T_{A_1} on the time-scale V_1/K_T. Since one needs to account for mixing through a deep layer in which stable stratification exists, this time-scale should be long in comparison to that of the 1–2 month period for the surface mixed layer noted above. Consequently, the restoring constant K_T is set equal to $3.5 \times 10^6\ \mathrm{m^3\,s^{-1}}$, which yields a restoring time-scale for the deep layer of O(75 years).

The precise choice for the deep-layer restoring time-scale is somewhat arbitrary, but does not qualitatively effect the dynamics, provided it is significantly less than the diffusive time-scale for salinity implied by eq. (9), in the limit for no advection. This requirement preserves the possibility of multiple steady states resulting from the circulation-salinity feedback mechanism (Stommel, 1961; Rooth, 1982), as will be shown below. The relatively long time-scale of 75 years means that high-frequency ocean modes (decadal time-scales and less) are not represented in the model. However, since the ocean model is highly averaged spatially, it is not possible to simulate the advective mechanisms responsible for these modes (Weaver and Sarachik, 1991) in any case. These limitations should be noted when the results from the coupled model simulations are presented in Section 5.

Eq. (6)–(12) are put into non-dimensional form by application of the following scaling:

$$T \to \frac{T}{T_0}, \qquad S \to \frac{\beta S}{\alpha T_0},$$

$$q \to \frac{q}{q^*}, \qquad t \to \frac{q^* t}{V_1 + V_2 + V_3},$$

where α and β are the coefficients of heat and salt expansion, respectively and T_0 and q^* are a reference temperature and thermohaline circulation. This results in the following, non-dimensional equations for the ocean model:

$$r_1 \frac{dT_1'}{dt'} = \frac{1}{2} q'(T_2' - T_3') + K_T'(T_{A_1}' - T_1') - K_{Z_1}'(T_1' - T_3'), \quad (14)$$

$$r_2 \frac{dT_2'}{dt'} = \frac{1}{2} q'(T_3' - T_1') + K_T'(T_{A_2}' - T_2') - K_{Z_2}'(T_2' - T_3'), \quad (15)$$

$$r_3 \frac{dT_3'}{dt'} = \frac{1}{2} q'(T_1' - T_2') + K_{Z_1}'(T_1' - T_3') + K_{Z_2}'(T_2' - T_3'), \quad (16)$$

$$r_1 \frac{dS_1'}{dt'} = \frac{1}{2} q'(S_2' - S_3') - K_{Z_1}'(S_1' - S_3') - Q_s', \quad (17)$$

$$r_2 \frac{dS_2'}{dt'} = \frac{1}{2} q'(S_3' - S_1') - K_{Z_2}'(S_2' - S_3') + Q_s', \quad (18)$$

$$r_3 \frac{dS'_3}{dt'} = \frac{1}{2} q'(S'_1 - S'_2) + K'_{Z_1}(S'_1 - S'_3) + K'_{Z_2}(S'_2 - S'_3), \tag{19}$$

where the prime denotes a non-dimensional variable and:

$$r_j = \frac{V_j}{V_1 + V_2 + V_3},$$

$$K'_T = \frac{K_T}{q^*}, \qquad K'_{Z_j} = \frac{K_{Z_j}}{q^*}$$

$$Q'_s = \frac{\beta Q_s}{\alpha T_0 q^*},$$

$$q' = \frac{\mu \alpha T_0}{q^*} [(T'_2 - T'_1) - (S'_2 - S'_1)].$$

Hereafter, the primes will be dropped when referring to non-dimensional variables; however, all results will be presented in terms of the dimensional equivalents except where the non-dimensional value is necessary for the elucidation of a particular point. Table 2 lists the values of the parameters used for all integrations of the ocean model.

By setting the left-hand sides of eqs. (14)–(19) to zero and expanding the resultant equations in powers of q one can derive a 5th-order equation describing the steady-state solutions of the ocean model:

$$q^5 + 4K_Z(K_T + K_Z)\, q^3 - 4\lambda K_Z Z q^2 + 16K_Z^3(K_T + K_Z)\, q + 32\lambda K_Z^2 K_T Q_s + 16\lambda K_Z^3 Z = 0, \tag{20}$$

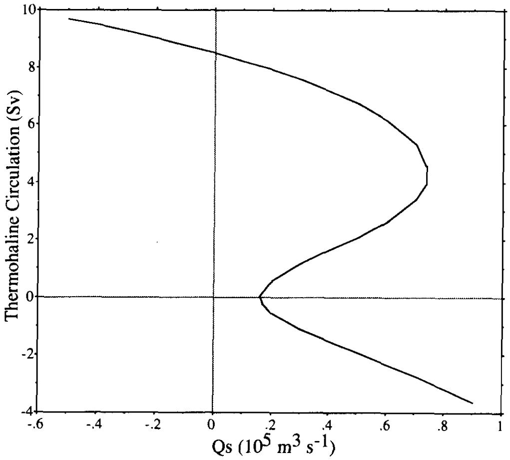

Fig. 3. The equilibrium solution for the thermohaline circulation ($1\ \mathrm{Sv} = 10^6\ \mathrm{m^3\ s^{-1}}$) as a function of Q_s for steady restoring temperatures ($T_{A_2} - T_{A_1} = 20°\mathrm{C}$).

where $K_Z = K_{Z_1} = K_{Z_2}$ and the buoyancy torque $Z = K_T(T_{A_2} - T_{A_1}) - 2Q_s$. The parameter λ is the constant of proportionality in the expression for non-dimensional q such that $\lambda = \mu\alpha T_0/q^*$.

Eq. (20) permits at most three real roots. Equilibrium solutions are plotted as a function of Q_s for fixed restoring temperatures in Fig. 3. The essence of the behavior is similar to Birchfield (1989) in that for small Q_s (positive buoyancy torque, differential heating dominant over evaporation), the flow is towards the North with relatively warm/saline surface waters and cold/fresh deep water (T and S not shown), while for large Q_s (negative buoyancy torque), the flow is reversed

Table 2. *Dimensional and equivalent non-dimensional ocean model constants*

Dimensional constant	Dimensional value	Non-dimensional constant	Non-dimensional value
V_1	$0.832 \times 10^{16}\ \mathrm{m^3}$	r_1	16.495
V_2	$2.592 \times 10^{16}\ \mathrm{m^3}$	r_2	5.295
V_3	$10.300 \times 10^{16}\ \mathrm{m^3}$	r_3	1.332
K_T	$3.5 \times 10^6\ \mathrm{m^3\ s^{-1}}$	K'_T	0.350
K_Z (diffusive)	$5.276 \times 10^5\ \mathrm{m^3\ s^{-1}}$	K'_Z	0.05276
K_Z (convective)	$5.276 \times 10^8\ \mathrm{m^3\ s^{-1}}$	K'_Z	52.76
q^*	$10 \times 10^6\ \mathrm{m^3\ s^{-1}}$	—	—
α	$9.622 \times 10^{-5}\ \mathrm{K^{-1}}$	—	—
β	7.755×10^{-4}	—	—
T_0	298.15 K	—	—
μ	$4 \times 10^{10}\ \mathrm{m^3\ s^{-1}}$	—	—

with a warm/saline deep ocean. However, for intermediate values of Q_s there exist multiple equilibria, corresponding to two positive (strong, weak) and one reversed thermohaline circulation. As will be shown in Subsection 4.2, it is in this intermediate region of Q_s that the time-dependent solutions also exhibit complex behavior.

4. The coupled model

4.1. Atmospheric coupling

The atmospheric model couples to the ocean model through the parameters F and G, corresponding to the meridional and zonal gradients in diabatic heating. One can relate changes in F and G directly to the temperatures in the upper ocean boxes, T_1 and T_2. As shown in Section 3, two basic equilibrium ocean states result from the box model dynamics, corresponding to warm, salty (q positive) and cold, fresh (q small or negative) high latitude waters. Thus, the warm, salty solution should result in a reduced meridional gradient in diabatic heating (F), while the zonal gradient in diabatic heating (G) should be increased (in winter), in association with the increased high latitude ocean temperatures. Correspondingly, the collapsed flow should lead to increased values of F and decreased values of G, in association with cooler high-latitude ocean temperatures. In order to associate G with T_1 in this way, there is an implicit assumption concerning the heating of the continent, namely, that a basic zonal gradient exists between the ocean and land regions (warmer land summer, colder land winter), upon which changes induced by fluctuations in the ocean temperature T_1 are superimposed.

The atmospheric coupling is then represented by allowing F and G to vary in a seasonal cycle upon which longer term variations associated with changes in the upper ocean temperatures are superimposed:

$$F(t) = F_0 + F_1 \cos \omega t + F_2(T_2 - T_1), \tag{21}$$

$$G(t) = G_0 + G_1 \cos \omega t + G_2 T_1, \tag{22}$$

where ω is the annual frequency and $t = 0$ at winter solstice. Making the assumption that the annual average F for a collapsed flow ($q \approx 0$, $T_1 \approx 0.944$, $T_2 \approx 0.993$) is of the order of the wintertime F for normal q, recognizing that for normal transport, $F_0 + F_2(T_2 - T_1) \approx 7$ units and letting $F_1 = 2$ yields $F_0 = 6.65$ and $F_2 = 47.9$. Making the further assumptions that the annual average G for a collapsed flow is order zero, and that for normal flow, $G = 1.32$ (-1.16) at winter (summer) solstice yields $G_0 + G_2 T_1 \approx 0.08$ units, $G_0 = -3.60$, $G_1 = 1.24$ and $G_2 = 3.81$.

These assumptions, while somewhat arbitrary, insure that F and G remain bounded by qualitatively plausible constraints for collapsed flows. In addition these assumptions insure that for normal ocean flow, F corresponds to the standard values of Lorenz (1984, 1990) while G attains a range that permits intransitive atmospheric behavior (active/inactive) in the summer and chaotic behavior in the winter (see Table 1 and Fig. 1). This range of G also permits transitory blocking to occur in either season when the seasonal cycles in F and G are included. This result seems reasonable, since transitory blocking is a fairly common occurrence in the real atmosphere (Rex, 1950ab; Treidl et al., 1981; Knox and Hay, 1985).

In Subsection 2.1, it was shown that the seasonal "climates" as defined by the atmospheric model attractors are quite distinct and the climate response to the ocean feedback can be highly complex. However, the coupling expressed by eqs. (21)–(22) results in what amount to very small variations in F and G for typical deviations of the ocean circulation about the normal value (corresponding to the strong positive equilibrium solution discussed in Section 3). For example, experience with the coupled model suggests that variations of q are on the order of 0.4 Sv; this yields correspondingly small deviations in the surface volume-averaged ocean meridional temperature gradient $T_2 - T_1$ (order 0.30°C) and high-latitude surface volume-averaged ocean temperature T_1 (order 0.13°C). Thus, the deviations in F (G) associated with these changes in the ocean circulation amount to 0.05 (0.002) units, in contrast to seasonal variations in F (G) of 4 (2.48) units. It is natural to ask whether these variations associated with the ocean circulation (which are 0.1 to 1% of the seasonal cycle) are significant?

The answer to this question for non-linear flows is not obvious. Frequently, it is difficult to seperate variations that are the result of specific causes from the larger natural variability, which for chaotic flow, may simply reflect a reorganization that is the consequence of "internal" rather than "external" forcing. However, it was shown in Subsection 2.2 that the dynamical behavior of the atmospheric model is highly complex within relatively narrow windows in F (for fixed G) and G (for fixed F); thus, the suggestion is that the relatively small variations resulting from adjustments in the ocean circulation might indeed be significant.

A direct attempt at answering this question was made by examining the behavior of eqs. (1)–(3) for small deviations about the "normal" F and G with a seasonal cycle superimposed. Fig. 4 shows the frequency of winter blocking, defined as the 100 year running average of blocking winters (where marginal and blocking winters are defined by 0.5 and 1, respectively, and a chaotic winter is 0; see Section 5 for specific definitions), for two pairs of F and G. The differences portrayed in the figure are illustrative of two important points. It is clear that there is significant "internal" long-term variability even for fixed values of F and G (as measured by the variation of blocking frequency along a given curve), a result that is consistent with recent work with eq. (1)–(3) by Pielke and Zeng (1994); further evidence will be presented in the next section. Although this "natural variability" is the dominant feature of the curves, specific differences in blocking frequency between the two $F-G$ pairs are also evident. A statistical test shows that the differences in the mean blocking frequency for the two $F-G$ pairs are significant at a very high level of confidence (well above 99%); that is, the differences in blocking frequency are not likely due to chance variation but rather reflect some fundamental difference in the "climate" of the two modes. Since F and G will undergo continuous incremental adjustments to changes in the ocean state as indicated by eqs. (21)–(22), an important feedback between the deep ocean circulation and climate is indeed possible. This ocean to climate feedback then initiates new changes in the ocean circulation (see Subsection 4.2 below) and so on. Furthermore, because of the non-linear nature of these mutual adjustments, any a priori predictions about the coupled system response are not possible.

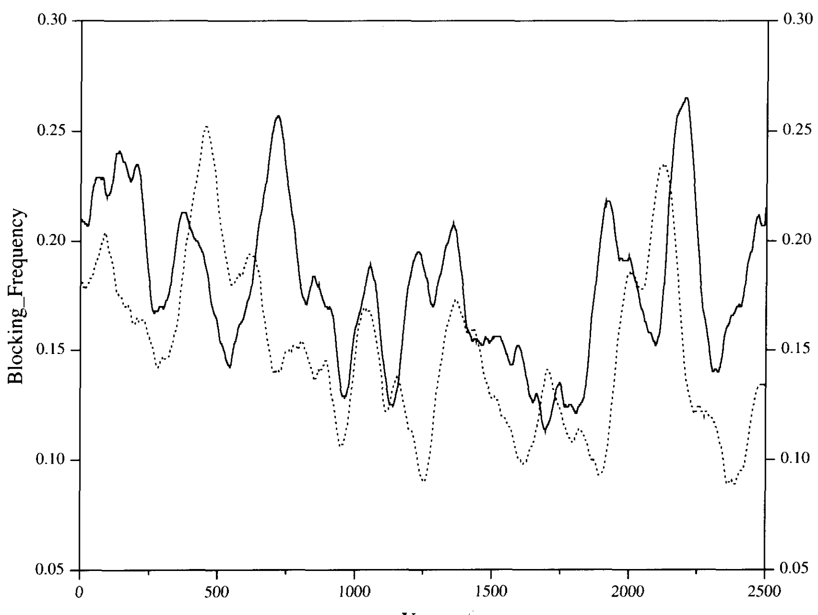

Fig. 4. 100-year centered moving average frequency of occurrence of winter blocking as a function of two seasonally varying $F-G$ pairs. The frequencies were obtained from continuous 2500-year integrations of the seasonal atmospheric model. The solid line is for $F = 8.975$ and $G = 1.321$, while the dashed line is for $F = 9.025$ and $G = 1.319$, both at winter solstice.

4.2. Ocean coupling

The ocean model couples to the atmospheric model through the restoring temperatures T_{A_1} and T_{A_2} and the equivalent salt flux (differential net surface evaporation) Q_s. Since X in the atmospheric model relates directly to the meridional temperature gradient, the restoring temperatures are defined by:

$$T_{A_1}(t) = T_{A_2} - \gamma X(t), \tag{23}$$

where γ and T_{A_2} are constants. Assuming that $T_{A_2} - T_{A_1} = 0.06708$ (20°C) for average (chaotic) winter conditions (with $X = 1.054$) and letting T_{A_2} remain fixed at 1.00 (25°C) yields $\gamma = 0.06364$.

The equivalent salt flux should be tied to the hydrological cycle, involving both river runoff and the atmospheric meridional transport of water vapor. The equivalent salt flux is then defined by:

$$Q_s(t) = Q_{\text{runoff}} + [Q_{\text{wv}}] + Q'_{\text{wv}} \tag{24}$$

where Q_{runoff} is that portion of the freshwater flux due to runoff from the rivers into the ocean basin and $[Q_{\text{wv}}]$, Q'_{wv} are proportional to the mean and transient eddy components of the total atmospheric water vapor transport, respectively.

Birchfield (1989) found a bifurcation point in his ocean model such that, for equivalent salt flux below a critical value, solutions displayed a damped oscillatory behavior, while higher values lead to amplifying vacillations and ultimately a complete flow reversal (Fig. 6 in Birchfield, 1989); in both cases, the solutions eventually attained a steady-state. The modified model presented here exhibits this same behavior, for intermediate values of Q_s. As shown in Fig. 5, this bifurcation point is near 0.0023 (0.23×10^5 m^3 s^{-1} in dimensional terms). Therefore, setting non-dimensional $Q_s = 0.0020$ for annual average conditions and using the facts that two-thirds of the net freshwater flux into the northern part of the North Atlantic is due to runoff (Broecker et al., 1990) and that approximately one-half of the total meridional water vapor transport at mid-latitudes is accomplished by the transient eddies (Peixoto and Oort, 1992, p. 285–293), eq. (24) is rewritten as:

$$Q_s(t) = 0.00166 + 0.00022(Y^2 + Z^2). \tag{25}$$

This parameterization is made possible by the further assumption that the eddy water vapor transport is directly proportional to the eddy sensible heat flux $Y^2 + Z^2$ (Stone and Yao, 1990).

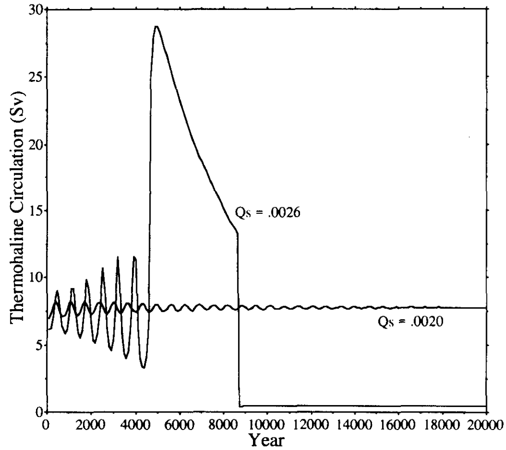

Fig. 5. The time-dependent thermohaline circulation for non-dimensional values of Q_s on either side of the solution bifurcation point.

A short time series of non-dimensional Q_s based upon this parameterization is shown in Fig. 6, for the uncoupled atmospheric model with seasonal cycles in F and G (eq. (21)–(22) with normal values for T_1 and T_2). Over seasonal time-scales, eq. (25) produces a pattern consistent with atmospheric observations, with relatively high values in winter and low values in summer (Peixoto and Oort,

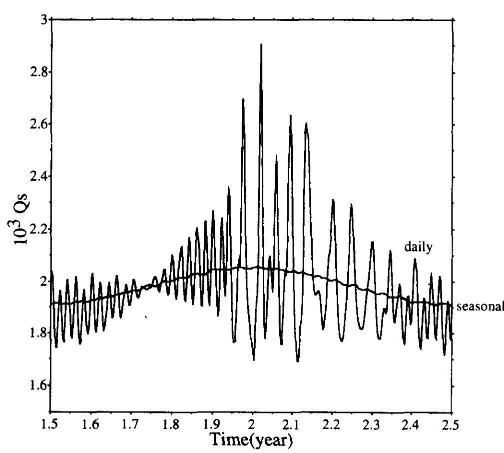

Fig. 6. Time-dependent behavior of Q_s as computed from the seasonal atmospheric model for a one year period (mid-summer to mid-summer). Shown are daily and seasonal values (obtained from a 90-day centered moving average).

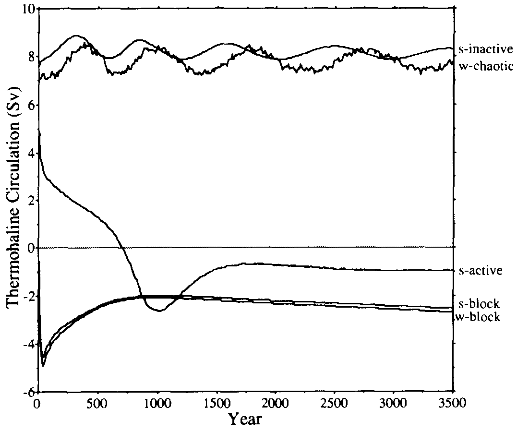

Fig. 7. The time-dependent thermohaline circulation for 3500 year integrations of perpetual atmospheric conditions. Shown are winter chaotic, winter/summer blocking, summer active and summer inactive conditions. See text for details.

1992). However, the "synoptic-scale" variability in Q_s is considerable, with fluctuations about the seasonal mean on the order of 10–50%. In numerical model simulations, Gutowski et al. (1992) found evidence for such episodic pulsing in the meridional moisture transport, related to the occurrence of rapid mid-level drying in the subtropics during eddy growth.

It is of interest to determine the response of the ocean model to different values of the temperature and salinity forcing corresponding to 5 cases of perpetual atmospheric conditions (winter chaotic, winter block, summer active, summer inactive, and summer block, respectively). Fig. 7 shows the time-dependent thermohaline circulations resulting from 3500 year integrations of the ocean model with the above perpetual atmospheric conditions. Three of the solutions (summer active/block and winter block) correspond to haline dominated circulations, in which the high equatorial salinity (relative to high latitudes) governs the hemispheric density gradient, leading to a collapse or reversal of the thermohaline circulation (i.e., equatorial deep water formation). The time-scale for these circulations to become well established is relatively shorter in the blocking cases than in the summer active condition (order 100 versus 1000 years). In reality, such ocean circulations have not been detected in either the Atlantic or in the global mean in the past 10^4–10^5 years. In contrast, the winter chaotic and summer inactive cases both lead to the more realistic positive circulations, with downwelling at high latitudes. Both of these cases display the damped oscillatory behavior discussed above for Q_s just below the bifurcation point.

The results of Figs. 5 and 7 suggest that "normal" conditions (chaotic winter, inactive summer) would be associated with a low-frequency oscillation in the ocean circulation, characteristic of an equivalent salt flux below the critical value. However, the feedbacks between the ocean and atmosphere must also be considered. For example, during the fast phase of the oscillation, T_1 (and S_1) will tend to increase in response to increased advection from low-latitudes. This increase in high-latitude ocean temperature would lead to a decrease in F (and an increase in wintertime G). As discussed in Subsection 4.1, these changes might then lead to an adjustment in the "climate", which would depend upon both the internal state of the atmospheric system and the external forcing represented by the change in the ocean circulation. If these changes lead to an increased frequency of winter blocking, this would reinforce high-latitude warming (through an increase in atmospheric heating or reduced cooling) but also oppose increasing salinity through freshening from precipitation. Both the warming and the freshening would tend to oppose the increase in the circulation by reducing the meridional density gradient (surface flow towards higher density, return flow at depth); thus, one might expect a subsequent adjustment towards cooler high-latitude ocean temperatures (advection reduced). These transitions between reasonably distinct climate patterns which are correlated with the phase of the ocean circulation might tend to damp the oscillations. On the other hand, a decrease in the frequency of winter blocking (in association with the fast phase of the oscillation) would oppose the high-latitude warming but reinforce increased salinity in that region, leading to even stronger ocean circulations.

A further complication must also be considered: the period required for the quasi-steady ocean circulations of Fig. 7 to develop is long (compared to atmospheric time scales) even for the most rapid case. For example, Fig. 8 shows the time series of the meridional temperature gradient X for a non-blocking and a major blocking winter. Because of the continued progression in F and G associated with the seasonal cycle, the solution resides in that

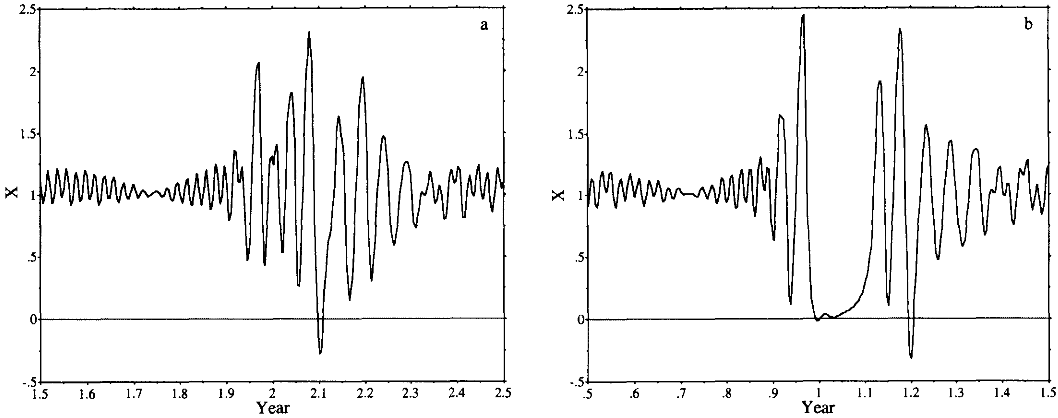

Fig. 8. Meridional temperature gradient (X) for (a) non-blocking and (b) major blocking winters from the seasonal atmospheric model.

part of the model phase space corresponding to blocking only for a short time (approximately 40 days, which is small relative to the ocean circulation time scales suggested by Fig. 7). As a result of such transitions, the overall impact of a winter block on the ocean circulation is reduced and the time scale for adjustment is correspondingly longer. In the case of the major blocking versus non-blocking winters shown in Fig. 8, the increase in the seasonal Q_s is approximately 2% (as compared to the 15% increase necessary to move from the damped oscillatory to collapsed flows shown in Fig. 5), while the increase in the high-latitude atmospheric temperature T_{A_1} is about 3% (8°C). Accordingly, to examine the long-term behavior of the ocean circulation and the associated climate, it is necessary to turn to experiments with the fully coupled model, which are presented in Section 5.

5. The coupled model experiments

Two 10000 year integrations of the ocean-atmosphere models were run, the first with complete coupling between the atmosphere and ocean models as described in Section 4, and the second in which F and G are decoupled from the thermohaline circulation (eqs. (21)–(22) with normal values of T_1 and T_2). These experiments will be referred to as the "coupled" and "uncoupled" model runs, respectively. A comparison of these runs will allow a determination of the effects of interactions between the atmosphere and ocean on the two climate subsystems in this simple model. The first 5000 years of the integrations are used to spin-up the coupled system: all results will be presented for the 5000 years following the spin-up interval.

Since three fundamental time-scales are associated with the ocean model (diffusive/convective, advective and restoring), one might expect a quasi-periodic type of behavior to emerge. The Fourier spectrum of a quasi-periodic function which depends non-linearly on three periodic functions of frequency f_i contains components at all frequencies of the form $m_1 f_1 + m_2 f_2 + m_3 f_3$ where m_i are arbitrary (small) integers (Bergé et al., 1984). Generally, the spectrum of the signal will be dense, but with higher power at various combinations of the fundamental frequencies. Of course, the situation is further complicated here by the fact that the advective time-scale is itself a function of the flow.

Fig. 9 shows the time-dependent response of the ocean circulation to the uncoupled and coupled atmospheric forcing. The uncoupled model results (Fig. 9a) show the low-frequency oscillatory behavior characteristic of one of the two basic modes of the ocean model (see Figs. 5 and 7); the fundamental frequency of these oscillations is 683 years, corresponding to the diffusive time-scale. In the coupled case (Fig. 9b), the ocean circulation again exhibits oscillatory behavior on a frequency which corresponds to the diffusive time-scale. However, an important distinction is the apparent additional power at higher frequencies.

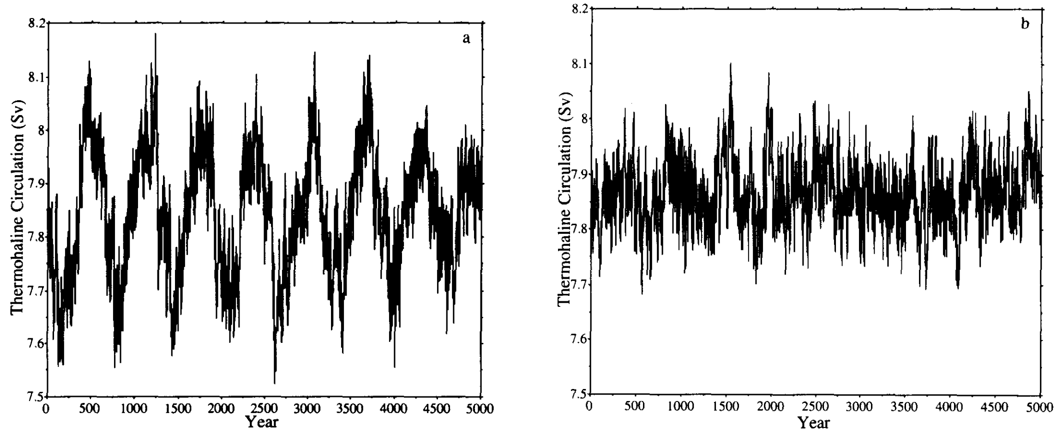

Fig. 9. The thermohaline circulation for 5000-year integrations (following a 5000-year spin-up) of the (a) uncoupled and (b) coupled model simulations. See text for details.

A spectral analysis of the two simulations reveals these distinctions more clearly. Both the uncoupled and coupled model ocean circulation data (Fig. 10) exhibit the dense power spectrum characteristic of a quasi-periodic signal, with the highest power at the diffusive time-scale (683 years). However, the coupled model data also show a greater extension of the power across a broad range of higher frequencies (i.e., 50–200 year period).

An examination of the low-frequency oscillations in the coupled model ocean circulation is revealing. As shown in Fig. 5, it is the equivalent freshwater flux Q_s that is responsible for such oscillations (although for *constant* Q_s below a critical value the oscillations gradually damp until a basin equilibrium is achieved). However, since in the coupled model simulation Q_s is also a function of the upper ocean temperatures through eqs. (21)–(22), an additional feedback can occur. Additional analysis is necessary to understand how this process affects the results.

The period from years 300–900 is marked by a complete oscillation in q, which falls to a minimum near year 650 below 7.7 Sv from a peak value near 8.1 Sv (Fig. 9b). Reference to eqs. (14)–(19)

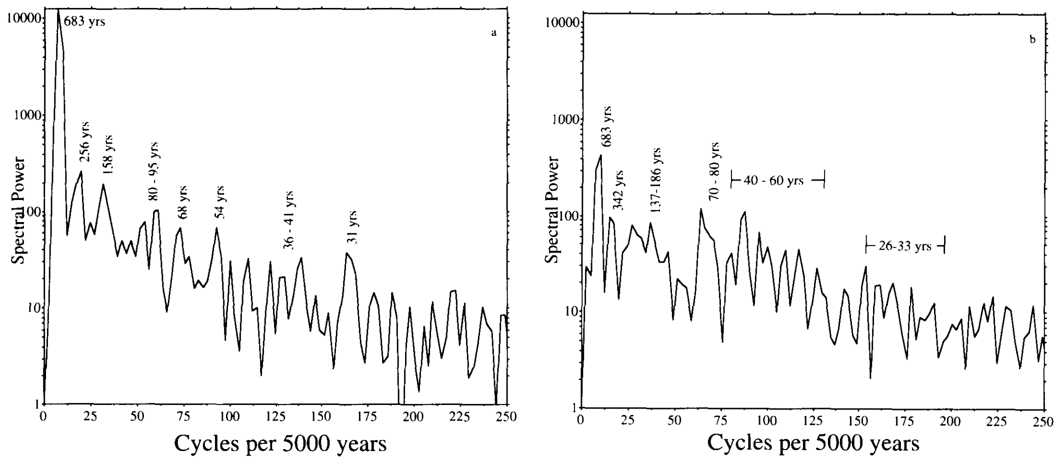

Fig. 10. Spectral analyses of the thermohaline circulation obtained from the integrations depicted in Fig. 9. Power spectra shown are for the (a) uncoupled and (b) coupled model simulations.

indicates how the oscillation is maintained. The oscillations of temperature and salinity are in phase in the surface boxes such that T_1 and S_1 decrease along with the decrease in q; at the same time T_2 and S_2 are past minimum and are beginning a commensurate increase. The amplitude of the oscillation is slightly larger in salinity than in temperature in box 1; in contrast, the amplitude of the oscillation is slightly larger in temperature than in salinity in box 2. Consequently, it is the relative changes in high-latitude salinity and low-latitude temperature that together govern the changes in the strength of the thermohaline circulation through the oscillation.

During the decreasing circulation phase, the upwelling of relatively cold deep water is reduced at low latitudes; this allows the heating of the surface waters by the overlying air to overcome diffusional losses to the deep ocean, and T_2 increases. The circulation then begins to strengthen as a result of the increased thermal component of the meridional density gradient, in combination with increases in high latitude salinity; the upwelling of deep water is then restored sufficiently to begin reducing the temperature of the low latitude surface waters. Eventually, this reduction of the thermal component of the meridional density gradient begins to weaken the circulation and the process begins anew.

However, this thermally-driven flow is also modified by changes in salinity. During the decreasing circulation phase (which is initially driven by reductions in low latitude temperature), decreases in S_1 occur concurrently because the diffusive losses into the deep ocean and freshening by surface fluxes are no longer balanced by gains through advection from low-latitudes. These salinity reductions reinforce the weakening of the circulation. Eventually, increases in high latitude salinity begin as a result of renewed advection from low latitudes (due in part to the reduced upwelling of relatively fresh water from the deep ocean, such that S_2 increases). S_1 and q then begin to increase until the advective contribution is sufficiently reduced by increased upwelling of deep water at low-latitudes, and the salinity process begins anew.

One might expect that certain preferred climates would be associated with particular phases of these low-frequency thermohaline circulation oscillations. It is possible to define specific winter and summer atmospheric patterns from the seasonal mean and variance of the meridional temperature gradient X. For example, Lorenz (1990) defined "inactive" and "active" summers on the basis of the standard deviation of X. Here, a similar procedure is employed (based upon an analysis of the time-dependent solutions of eqs. (1)–(3) with seasonal F and G) to define the following patterns: winter "block", winter "marginal-block", winter "chaotic", summer "block", summer "inactive", summer "active" as follows:

winter block: $[X_W] \leqslant 0.85$

winter marginal-block: $0.85 < [X_W] \leqslant 0.90$

winter chaotic: $[X_W] > 0.90$

summer block: $[X_S] \leqslant 0.90$

summer inactive: $[X_S] > 0.90$ and $\sigma(X_S) < 0.3$

summer active: $[X_S] > 0.90$ and $\sigma(X_S) \geqslant 0.3$,

where $[X_W]$, $[X_S]$ are the seasonal means of X for the winter and summer seasons, respectively and σ is the standard deviation of X for the indicated season. The subdivision of winter blocking is necessary to differentiate between winters with rapid transitory blocking episodes (marginal-block, order 1 week) and those with more extended periods of blocking (order 1 month; see Fig. 8). Using these definitions, it should be possible to obtain some insight into the variability of the "climate" as a function of changes in the ocean circulation.

As a point of reference, Table 3 gives a summary

Table 3. *Summary of the "climate" derived from the coupled and uncoupled atmosphere-ocean model simulations (5000 years); numbers are the frequency of occurrence, expressed as a percentage*

Simulation	Winter block	Winter marginal block	Winter chaotic	Summer inactive	Summer active	Summer block
coupled	1.7	28.7	69.6	89.9	10.1	0.1
uncoupled	14.6	26.7	58.7	65.2	34.0	0.8
difference	−12.9	+2.0	+10.9	+24.7	−23.9	−0.7

Table 4. *Summary of the "climate" of the low-frequency oscillatory phases (bottom 10% and top 90%) of the coupled model simulation; numbers are the frequency of occurrence, expressed as a percentage*

Phase	Winter block	Winter marginal block	Winter chaotic	Summer inactive	Summer active	Summer block
slow $q < 7.79$ Sv	2.8	49.0	48.2	91.0	8.8	0.2
fast $q > 7.95$ Sv	0.8	10.5	88.7	90.9	9.1	0.0
difference	+2.0	+38.5	−40.5	+0.1	−0.3	+0.2

of the climate so-defined, but for the full 5000 years of the coupled and uncoupled model runs. Overall, winter climates are characterized by chaotic conditions with frequent interludes of blocking. The summer climate is generally inactive, but occurrences of the active/block modes are not rare. The main effect of coupling on the overall climate is to increase the frequencies of chaotic winters and inactive summers; this has the effect of moderating the ocean circulation oscillations (Fig. 9), by reducing the frequency of atmospheric modes associated with thermohaline collapse (see Fig. 7).

Table 4 presents the climate conditions associated with the slow and fast phases of the low-frequency ocean circulation oscillations. Comparison with Table 3 shows that there is little distinction between the summer patterns associated with these oscillation phases. However, during the slow phases, winter blocks become more frequent and extended while during the fast phases, winters are characterized by chaotic conditions with infrequent blocking transitions. Furthermore, the residence time in each phase of the oscillation (slow-transition-fast-transition-slow) is order 100–300 years. Such clear temporal distinctions in real-world statistics would almost certainly be interpreted as climatic change.

The high-frequency spectral power noted above in the coupled model ocean circulation corresponds to oscillations of order 0.2 Sv. Examples of such oscillations are shown in Fig. 11, for the years 900–1100, corresponding to the fast-mode in the low-frequency ocean circulation. During this period, T_1 undergoes high-frequency oscillations which are superimposed upon a slowly evolving trend. S_1 changes in concert with the slow evolution of T_1, while T_2 and S_2 undergo slow concurrent modulations. Consequently, the main

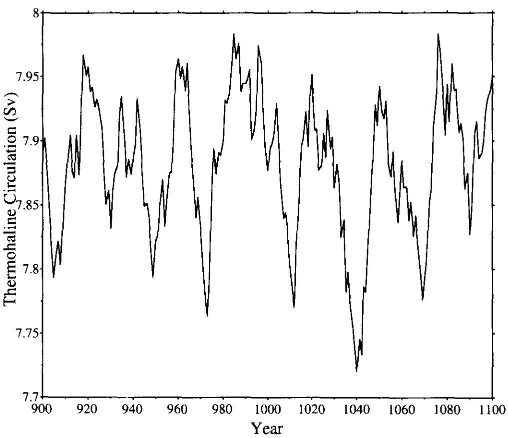

Fig. 11. Thermohaline circulation for the years 900–1100 from the coupled model simulation.

contribution to the high-frequency variations in q is from temperature changes in the high-latitude surface box. These oscillations, arising due to thermal imbalances between the advective and restoring terms of eq. (14), are a direct response to similar periodicities in the atmospheric signal (see below). Although the magnitude of these high-frequency ocean oscillations is small, it does not follow that they are necessarily insignificant in terms of the impact on the climate. As discussed in Section 4, the atmospheric model is quite sensitive in certain regions of $F-G$ space to small changes in position; consequently, the response in some cases might be fluctuations between different predominant climates.

Consider the thermohaline oscillation beginning at the circulation minimum near year 970 and increasing to a peak value near year 990. In year 970, following a series of marginal blocking

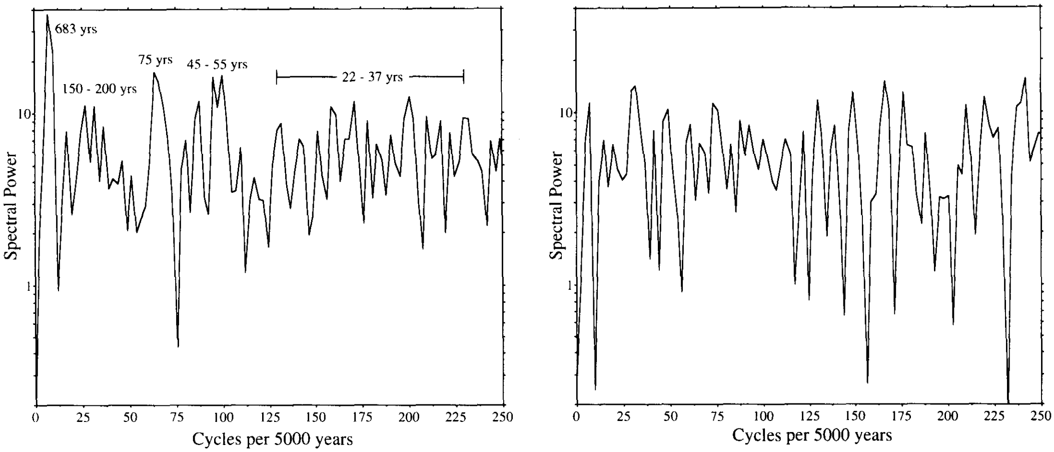

Fig. 12. Spectral analysis of $[X_w]$ obtained from the (a) coupled and (b) uncoupled model simulations.

winters, the temperature in the high-latitude surface ocean is relatively warm and the ocean circulation is correspondingly slow. However, once the climate shifts to a higher frequency of chaotic winters, the high-latitude surface ocean cools and the circulation increases. This increased circulation leads to stronger advection of the warm equatorial surface waters to high-latitudes, which eventually balances the losses to the (now colder) atmosphere near year 990. Since the restoring temperature T_{A_1} is directly related to the meridional temperature gradient X through eq. (23), a spectral analysis of X_w for the coupled model simulation is shown in Fig. 12a. Comparison with Fig. 10b suggests that the 20–50 year variations in X_w are responsible for a significant proportion of the high-frequency oscillations in q throughout the coupled simulation.

Table 5 summarizes the climate conditions associated with the slow and fast phases of the high-frequency thermohaline circulation oscillations shown in Fig. 11. The distinction between the climates during both phases of the oscillation is clear; the prime modulating factor is the relative frequency of the marginal winter blocking modes and their corresponding effect on high-latitude temperatures.

A spectral analysis of X_w for the uncoupled model simulation is presented in Fig. 12b. Comparison of Figs. 12a and b reveals the preferential increase in power at the lowest frequencies in the coupled model simulation, consistent with the influence of the low-frequency oscillations in the thermohaline circulation suggested by Table 4. This is a broad demonstration of the argument of Hasslemann (1976): the "white-noise" atmospheric signal is converted by the slow (ocean)

Table 5. *Summary of the "climate" derived from a high-frequency oscillatory portion (bottom and top 25%) of the coupled model simulation (years 900–1100); numbers are the frequency of occurrence, expressed as a percentage*

Phase	Winter block	Winter marginal block	Winter chaotic	Summer inactive	Summer active	Summer block
slow $q < 7.85$ Sv	0.0	56.0	44.0	80.0	20.0	0.0
fast $q > 7.93$ Sv	0.0	11.9	88.1	78.6	21.4	0.0
difference	0.0	+44.1	−44.1	+1.4	−1.4	0.0

component of the climate system into higher variance "red-noise". There are also indications of a general shifting of high-frequency power into the lower frequencies (30–75 years), consistent with the linkage of the atmosphere-ocean interactions with preferred climate regimes at interdecadal time scales.

6. Discussion

In this paper, the dynamic behavior of the climate system is investigated through the use of a low-order coupled atmosphere-ocean general circulation model. The goal of this investigation has been to gain some qualitative understanding of how the subtle (non-linear) interactions between the individual system components may affect the climate. This subtlety is the result of the complexity of the atmospheric response to changes in the meridional and zonal gradients in diabatic heating, which are in part tied to the deep ocean circulation; the ocean circulation must then adjust to new patterns of atmospheric forcing, closing the feedback loop.

Although the ocean model eventually settles into two basic equilibrium responses to perpetual atmospheric conditions (steady positive and collapsed flows) such equilibrium states are never attained in the coupled system (at least within 10000 years), since the deep ocean flow must continually adjust to the atmospheric regime changes associated with particular ocean circulations, which ultimately leads to new circulations and new atmospheric regimes. Low frequency quasi-periodic oscillations in the deep ocean flow are forced by the interplay between surface fluxes (of freshwater and heat) and the advective-diffusive process; these oscillations are modulated by the correlation of the atmospheric behavior with the phase of the ocean cycle.

The climate is strongly effected by interactions with the ocean, leading to distinct atmospheric patterns for different phases of the ocean oscillations, and a conversion of some of the high-frequency atmospheric signal to lower-frequencies. The result that the interdecadal oscillations of the coupled simulation are primarily generated by the atmosphere is mandated by the simplicity of the ocean model. As discussed in Section 3, the advective mechanisms responsible for the high frequency ocean modes are not representable in this model. However, owing to the richness of the atmospheric response to small modifications in the meridional and zonal gradients in diabatic heating, even modest high-frequency adjustments in the ocean circulation induced by interactions with the high-frequency atmospheric component can also lead to climate change over relatively short time periods (30–75 year periods).

Naturally one may well ask what such model results can reveal about the real world? The utility of such low-order model studies of complex systems like the climate is in their ability to highlight the character of the non-linear response in a much more rigorous manner than is afforded by qualitative reasoning alone. Thus, the present model should be considered as a climate-dynamics thinking tool; the results presented here can be used to provide additional insight into the results obtained from more complex models and observations.

For instance, Greenland ice core data have recently become available which offer considerable information on observed temperature variability on the interdecadal to millenial time scales (GRIP Project Members, 1993; Dansgaard et al., 1993; Grootes et al., 1993; Taylor et al., 1993). These data suggest that there have been rapid transitions between warm and cold climates in the North Atlantic during the past 100,000 years or so. These mode switches may have occurred over periods as short as a few decades and remained fixed for periods ranging from 70 years to 5000 years. Atmospheric temperature changes associated with these transitions may have been as much as 10°C. Taylor et al. (1993) noted that these fluctuations were likely part of a larger atmospheric pattern that extended over the North Atlantic and Northwest Europe, reflecting forcing by the North Atlantic Ocean.

The model results presented here suggest that the low-frequency circulation-salinity feedback mechanism, modulated by the linkage of the atmosphere to the phase of the ocean cycle, can qualitatively mimic this observed behavior. The time-scale for this process is quasi-periodic; superimposed upon the basic diffusive time-scale of the system are the higher frequencies resulting from advection (which is itself a function of the flow) and higher-order atmospheric components. Thus, spectral peaks occur in the range of interdecadal to millenial time-scales. It is the coupling of the atmosphere with the ocean that allows the system to adjust relatively rapidly.

For example, consider the low-frequency oscillation in the thermohaline circulation (between the years 300–900) discussed in Section 5. A mode switch from a fast to a slow thermohaline flow was already underway as a result of increased upwelling of cold waters in the low-latitude surface box, a process which occurs on the diffusive time-scale. However, the transition to the slow mode was forced over a shorter (50 year) period by increased atmospheric blocking and corresponding decreases in high-latitude salinity, reinforcing the already weakening meridional density gradient. This transition in the thermohaline flow was accompanied by an equally rapid adjustment in high-latitude atmospheric temperatures. Once the rapid transition was completed, the diffusive time-scale for restoration of the thermohaline circulation required that the changed climate (see Table 4) remain in place for several hundred years. In order to test whether this mechanism could be responsible for the observed climatic transitions in the ice-core data, one would need information that could reveal the density structure of the Atlantic Ocean and some measure of the equivalent salt flux forcing during these intervals. Experiments with a high resolution, synchronously coupled atmosphere-ocean general circulation model might also provide some insight concerning the viability of this mechanism for more realistic conditions.

Also of considerable interest is the deduction from the Greenland ice-core data that the climate of the present (Holocene) interglacial period has been much more stable than that of the last (Eemian) interglacial period. The available evidence also suggests that the Eemian interglacial was somewhat warmer than today (GRIP, 1993). There is some basis from both observations and general circulation model experiments for concluding that a warmer climate would be associated with an enhanced hydrological cycle (Peixoto and Oort, 1992, p. 287–291; Manabe and Stouffer, 1993). Within the context of the present model, since higher amplitude oscillations in the ocean circulation are driven by a larger equivalent salt flux (to the limit of a flow bifurcation; see Fig. 5), one could argue that a reduction in equivalent salt flux might have taken place between the Eemian and Holocene interglacials as a result of the cooler present-day climate and that this reduction in equivalent salt flux has lead to the stability of the present interglacial period. Again, observational evidence of changes in the equivalent salt flux in combination with detailed modelling studies are needed to verify this scenario.

One advantage of a simple system such as the coupled model presented in this paper is that a detailed analysis of the dynamics can be made. In particular, it may be possible to gain some additional insight into the parameter dependence of the model solutions by performing a bifurcation analysis of the system. For example, what is the full parameter dependence of the two equilibrium ocean circulation solutions depicted in Fig. 5? What parameters (other than equivalent salt flux) may govern the time-dependent transitions between the two modes? Once a transition between modes is established (say, to a thermohaline collapse), can the original mode be reestablished? Such an analysis is beyond the scope of the present study, but will be undertaken in a future paper.

The results of such studies might be used to support the formulation of more complex modelling efforts. For instance, the thermohaline circulation in the present study is limited to a single basin; this has allowed a study of the interaction of an *Atlantic-type* deep circulation with a dynamic atmosphere. Inclusion of more basins would allow a simulation of the present day global "conveyor belt" (Gordon, 1986), as well as a variety of instability processes that could lead to transitions between different equilibria. Such a goal could be achieved within the constraints of the ocean box model dynamics, as shown by Marotzke (1990) and Wang and Birchfield (1992). The atmospheric component could be likewise expanded, perhaps by incorporating parallel versions of the Lorenz (1984) model. Although such an expansion would require a two to three-fold increase in the number of time-dependent equations, the level of simplicity would still be sufficient to allow a practical exploration of the dynamics of the coupled system.

An important component of the climate system for time-scales of order 10^3 to 10^4 years that has been neglected in this study is the cryosphere. In particular, interactions with the atmosphere and ocean through polar ice formation and melting might have substantial time-dependent effects on solar forcing (eq. (21)) through changes in reflectivity, and equivalent salt fluxes (eq. (25)) through runoff and the export of sea-ice to the North Atlantic (Aagaard and Carmack, 1989). A low-order approach to ice-sheet dynamics could be attempted, for example, following the work of Wertman (1964, 1976) and Källén et al. (1979). Such modifications to the current model might allow for a more thorough investigation of the climate sub-system interactions during glacial and interglacial periods, and the possible modes of transition between these states.

7. Acknowledgements

This research was inspired by numerous seminars and discussions held at the McGill University Centre for Climate and Global Change Research while the author was a doctoral student. Discussions with A. Weaver, W. Gough, D. Wright and G. Lesins and the comments of the anonymous reviewers were particularly enlightening and constructive. Many thanks are also due to L. Bosart for allowing me the freedom to continue this research while at SUNY.

REFERENCES

Aagaard, K. and Carmack, E. C. 1989. The role of sea–ice and other fresh water in the Arctic circulation. *J. Geophys. Res.* **94**, 14485–14498.

Bergé, P., Pomeau, Y. and Vidal, C. 1984. *Order within chaos. Towards a deterministic approach to turbulence.* John Wiley and Sons, New York, 329 pp.

Birchfield, G. E. 1989. A coupled ocean-atmosphere climate model: temperature versus salinity effects on the thermohaline circulation. *Clim. Dyn.* **4**, 57–71.

Birchfield, G. E., Wang, H. and Wyant, M. 1990. A bimodal climate response controlled by water vapor transport in a coupled ocean-atmosphere box model. *Paleoceanography* **5**, 383–395.

Blackmon, M. L., Mullen, S. L. and Bates, G. T. 1986. The climatology of blocking events in a perpetual January simulation of a spectral general circulation model. *J. Atmos. Sci.* **43**, 1379–1405.

Broecker, W. S., Puang, T.-H., Jouzel, J. and Russell, G. 1990. The magnitude of global freshwater transports of importance to ocean circulation. *Clim. Dyn.* **4**, 73–79.

Bryan, F. 1986a. High latitude salinity effects and inter-hemispheric thermohaline circulations. *Nature* **323**, 301–304.

Bryan, F. 1986b. *Maintenance and variability of the thermohaline circulation.* PhD thesis, Princeton University, Princeton, New Jersey, 254 pp.

Cox, M. D. 1984. *A primitive equation, three-dimensional model of the ocean.* GFDL Ocean Group Tech. Rep. No. 1.

Dansgaard, W., Johnsen, S. J., Clausen, H. B., Dahl-Jensen, D., Gundestrup, N. S., Hammer, C. U., Hvidberg, C. S., Steffensen, J. P., Sveinbjörnsdottir, A. E., Jouzel, J. and Bond, G. 1993. Evidence for general instability of past climate from a 250-kyr ice-core record. *Nature* **364**, 218–220.

Gordon, A. L. 1986. Interocean exchange of thermocline water. *J. Geophys. Res.* **91**, 5037–5046.

Greenland Ice-core Project (GRIP) Members, 1993. Climate instability during the last intergalcial period recorded in the GRIP ice core. *Nature* **364**, 203–207.

Grootes, P. M., Stuiver, M., White, J. W. C., Johnsen, S. and Jouzel, J. 1993. Comparison of oxygen isotope records from the GISP2 and GRIP Greenland ice cores. *Nature* **366**, 552–554.

Gutowski, W. J., Branscome, L. E. and Stewart, D. A. 1992. Life cycles of moist baroclinic eddies. *J. Atmos. Sci.* **49**, 306–319.

Harvey, L. D. D. 1992. A two-dimensional ocean model for long-term climatic simulations: Stability and coupling to atmosphere and sea–ice models. *J. Geophys. Res.* **97**, 9435–9453.

Hasselmann, K. 1976. Stochastic climate models. Part I. Theory. *Tellus* **28**, 473–485.

Hasselmann, K. 1982. An ocean model for climate variability studies. *Progr. Oceanogr.* **11**, 69–92.

Holton, J. R. 1992. *An introduction to dynamic meteorology*, 3rd edition, Academic Press, San Diego, 511 pp.

Källén, E., Crafoord, C. and Ghil, M. 1979. Free oscillations in a climate model with ice-sheet dynamics. *J. Atmos. Sci.* **36**, 2292–2303.

Källén, E. and Huang, X.-Y. 1987. A simple model for large-scale thermohaline convection. *Dyn. Atm. Oceans* **11**, 153–173.

Knox, J. L. and Hay, J. E. 1985. Blocking signatures in the Northern Hemisphere: Frequency distribution and interpretation. *J. Clim.* **5**, 1–16.

Lorenz, E. N. 1982. Low-order models of atmospheric circulations. *J. Meteor. Soc. Jap.* **60**, 255–267.

Lorenz, E. N. 1984. Irregularity. A fundamental property of the atmosphere. *Tellus* **36A**, 98–110.

Lorenz, E. N. 1990. Can chaos and intransitivity lead to interannual variability? *Tellus* **42A**, 378–389.

Manabe, S. and Stouffer, R. J. 1993. Century-scale effects of increased atmospheric CO_2 on the ocean-atmosphere system. *Nature* **364**, 215–218.

Marotzke, J., Welander, P. and Willebrand, J. 1988. Instability and multiple steady states in a meridional-plane model of the thermohaline circulation. *Tellus* **40A**, 162–172.

Marotzke, J. 1990. *Instabilities and multiple equilibria of the thermohaline circulation.* PhD thesis, Institut für Meereskunde, Christian-Albrechts-Universitat, Kiel, FRG, 126 pp.

Marotzke, J. and Willebrand, J. 1991. Multiple equilibria of the global thermohaline circulation. *J. Phys. Oceanogr.* **21**, 1372–1385.

Masoller, C., Sicardi-Schifino, A. C. and Romanelli, L. 1992. Regular and chaotic behavior in the new Lorenz system. *Phys. Lett.* **167A**, 185–190.

Mikolajewicz, U. and Maier-Reimer, E. 1990. Internal secular variability in an ocean general circulation model. *Climate Dynamics* **4**, 145–156.

Mullen, S. L. 1986. The local balances of vorticity and heat for blocking anticyclones in a spectral general circulation model. *J. Atmos. Sci.* **43**, 1406–1441.

Palmén, E. and Newton, C. W. 1969. *Atmospheric circulation systems: Their structure and physical interpretation.* Academic Press, New York, 603 pp.

Peixó to, J. P. and Oort, A. H. 1992. *Physics of climate.* American Institute of Physics, New York, 520 pp.

Pielke, R. A. and Zeng, X. 1994. Long-term variability of Climate. *J. Atmos. Sci.* **51**, 155–159.

Raethjen, P. 1949. Zyklogenetische probleme. *Arch. Meteorol., Geophys. Bioklimatol.* **A1**, 295–346.

Rex, D. F. 1950a. Blocking action in the middle troposphere and its effect upon regional climate. (I). An aerological study of blocking action. *Tellus* **2**, 196–211.

Rex, D. F. 1950b. Blocking action in the middle troposphere and its effect upon regional climate. (II). The climatology of blocking action. *Tellus* **2**, 275–301.

Rooth, C. 1982. Hydrology and ocean circulation. *Progr. Oceanogr.* **11**, 131–149.

Stocker, T. F., Wright, D. G. and Mysak, L. A. 1992. A zonally averaged, coupled ocean-atmosphere model for paleoclimate studies. *J. Climate* **5**, 773–797.

Stommel, H. 1961. Thermohaline convection with two stable regimes of flow. *Tellus* **13**, 224–230.

Stone, P. H. and Yao, M.-S. 1990. Development of a two-dimensional zonally averaged statistical-dynamical model. Part III: The parameterization of the eddy fluxes of heat and moisture. *J. Climate* **3**, 726–740.

Taylor, K. C., Hammer, C. U., Alley, R. B., Clausen, H. B., Dahl-Jensen, D., Gow, A. J., Gundestrup, N. S., Klpfstuhl, J., Moore, J. C. and Waddington, E. D. 1993. Electrical conductivity measurements from the GISP2 and GRIP Greenland ice cores. *Nature* **366**, 549–552.

Treidl, R. A., Birch, E. C. and Sajecki, P. 1981. Blocking action in the Northern Hemishpere: A climatological study. *Atmos.-Ocean* **19**, 1–23.

Wang, H. and Birchfield, G. E. 1992. An energy-salinity balance climate model. Water vapor transport as a cause of changes in the global thermohaline circulation. *J. Geophys. Res.* **97**, 2335–2346.

Weaver, A. J. and Sarachik, E. S. 1990. On the importance of vertical resolution in certain ocean general circulation models. *J. Phys. Oceanogr.* **20**, 600–609.

Weaver, A. J. and Sarachik, E. S. 1991. Evidence for decadal variability in an ocean general circulation model: An advective mechanism. *Atmosphere-Ocean* **29**, 197–231.

Weaver, A. J. and Hughes, T. M. C. 1992. Stability and variability of the thermohaline circulation and its link to climate. *Trends in physical oceanography.* Council of Scientific Research Integration, Research Trends Series, Trivandrum, India.

Welander, P. 1982. A simple heat-salt oscillator. *Dyn. Atm. Oceans* **6**, 233–242.

Wertman, J. 1964. Rate of growth or shrinkage of non-equlibrium ice-sheets. *J. Glaciol.* **6**, 145–158.

Wertman, J. 1976. Milankovitch solar radiation variations and ice-age ice sheet sites. *Nature* **261**, 17–20.

Wolf, A., Swift, J. B., Swinney, H. L. and Vastano, J. A. 1985. Determining Lyapunov exponents from a time series. *Physica* **16D**, 285–317.

Wright, D. G. and Stocker, T. F. 1991. A zonally averaged ocean model for the thermohaline circulation. Part I: Model development and flow dynamics. *J. Phys. Oceanogr.* **21**, 1713–1724.